Reconfigurable spin-wave non-reciprocity induced by dipolar interaction in a coupled ferromagnetic bilayer

Gallardo, R. A.; Schneider, T.; Chaurasiya, A. K.; Oelschlägel, A.; Arekapudi, S. S. P. K.; Roldáan-Molina, A.; Hübner, R.; Lenz, K.; Barman, A.; Fassbender, J.; Lindner, J.; Hellwig, O.; Landeros, P.;

Originally published:

September 2019

Physical Review Applied 12(2019), 034012

DOI: https://doi.org/10.1103/PhysRevApplied.12.034012

Reconfigurable spin-wave non-reciprocity induced by dipolar interaction in a coupled ferromagnetic bilayer

R. A. Gallardo,[1,2] T. Schneider,[3] A. K. Chaurasiya,[4] A. Oelschlägel,[3,5] S. S. P. K. Arekapudi,[6] A. Roldán-Molina,[7] R. Hübner,[3] K. Lenz,[3] A. Barman,[4] J. Fassbender,[3,5] J. Lindner,[3] O. Hellwig,[3,6,*] and P. Landeros[1,2,†]

[1] *Departamento de Física, Universidad Técnica Federico Santa María, Avenida España 1680, Valparaíso, Chile*
[2] *Center for the Development of Nanoscience and Nanotechnology (CEDENNA), 917-0124 Santiago, Chile*
[3] *Helmholtz-Zentrum Dresden-Rossendorf, Institute of Ion Beam Physics and Materials Research, Bautzner Landstr. 400, 01328 Dresden, Germany*
[4] *Department of Condensed Matter Physics and Material Sciences, S. N. Bose National Centre for Basic Sciences, Block JD, Sec. III, Salt lake, Kolkata 700106 India*
[5] *Technische Universität Dresden, Institute of Materials Science, 01062 Dresden, Germany*
[6] *Chemnitz University of Technology, Institute of Physics, 09126 Chemnitz, Germany*
[7] *Universidad de Aysén, Ovispo Vielmo 62, Coyhaique, Chile*

Frequency non-reciprocity of wave phenomena describes the situation where wave dispersion depends on the sign of the wave-vector, i.e., counter-propagating waves exhibit different wavelengths for the same frequency. Such behavior has been recently observed in heavy-metal/ferromagnetic interfaces with Dzyaloshinskii-Moriya coupling, and has also been known for coupled magnetic bilayers, where non-reciprocity is enhanced when the two layers are antiparallel aligned. Besides the conventional uses of spin-waves, non-reciprocity adds further functionalities, such as its potential applications in communications technologies and logical operations. In the current manuscript, we thus examine the spin-wave non-reciprocity induced by dipolar interactions in a coupled bilayer consisting of two ferromagnetic layers separated by a non-magnetic spacer. We derive an easy-to-use formula to estimate the frequency difference provided by the non-reciprocity, which allows for choosing an optimal system in order to maximize the effect. For small wave-numbers, non-reciprocity scales linearly, while for larger wave-vectors the non-reciprocity behaves non-monotonically, with a well-defined maximum. The study is carried out by means of analytical calculations that are complemented by micromagnetic simulations. Furthermore, we confirmed our model by experimental investigation of the spin-wave dispersion in a prototype antiparallel-coupled bilayer system. Since the relative magnetic orientation can be controlled through a bias field, the magnon non-reciprocity can be then turned on and off, which lends an important functionality to the coupled ferromagnetic bilayers.

I. INTRODUCTION

The engineering of spin waves (SWs)—the elementary excitations in magnetic systems with coupled electron spins—in magnetic structures attracts a lot of attention in the scientific community, motivated by applications based on the field of magnon-spintronics [1], which also provides a rich playground to study fundamental principles of magnetic wave phenomena [2–9]. Since SW frequencies can vary from GHz to THz and can be externally controlled by applying magnetic fields or by designing the system architecture to create desired magnonic properties, devices for high-frequency applications and data processing are envisioned [10–17]. In the context of data processing, the non-reciprocity of spin waves, which can appear in the phase, amplitude or frequency, is presented as a powerful tool for possible applications in communications and logic devices [18–20]. Non-reciprocal phenomena were in the focus of studies on photonic and electronic structures as well, for which they were found to enable fundamental operation modes in devices such as isolators, circulators or gyrators [21, 22]. Similarly, non-reciprocal magnon transport yields these key functionalities as well [18]. Consequently, achieving non-reciprocity in the spin-wave dispersion up to a significant, ideally tunable, degree is of high relevance for magnon-based applications.

Spin-wave non-reciprocity has been known since the pioneering work of Damon and Eshbach [23], where it was predicted that the magnetization precession amplitude of the surface mode should be asymmetric with respect to the propagation direction. Such behavior is well known and has been experimentally measured by several authors [24–26]. However, the amplitude non-reciprocity itself does not imply non-reciprocity in frequency. In our current bilayer case a symmetry breaking along the thickness will induce a frequency shift of two counter-propagating waves. The spin-wave frequency non-reciprocity has already been discussed in ferromagnetic (FM) films with different magnetic anisotropies at the surfaces [27–32], and films with interband magnonic transitions [33]. It has been moreover theoretically and experimentally demonstrated that the interfacial Dzyaloshinskii-Moriya interaction (DMI) [34–37] induced in ultrathin FM layers capped with heavy-metal films, noticeably influences the SW spectra, generating a non-reciprocity in the dispersion [38–54]. Additionally, non-reciprocal properties in FM materials can be introduced

* o.hellwig@hzdr.de
† pedro.landeros@usm.cl

by the intrinsic dipolar interactions. It was reported that arrays of magnetic nanopillars coupled by dipolar interaction [55], ferromagnetic nanotubes [56], systems composed by an FM film exchange-coupled to a one-dimensional periodic structure [57, 58] and antiferromagnetic trilayers [59, 60] show SW non-reciprocity. Although the physical properties of magnetic multilayers were extensively studied in the past decades, the focus was put on the celebrated giant change of magnetoresistance with the relative magnetic orientation of adjacent FM layers [61–63]. Interestingly, early studies of double- and multilayers by Brillouin light scattering (BLS) already evidenced frequency non-reciprocity for antiparallel alignment of the magnetic layers [64–68], in agreement with theoretical works [18, 69–73]. However, a theory with the potential of making specific predictions is so far still missing, which hinders establishing advantages and/or disadvantages of specific systems in comparison to others.

In this paper, the spin-wave dynamics of a FM bilayer system is investigated using a theoretical model, micromagnetic simulations and BLS experiments. By analyzing both, the magnetic properties of each layer and their equilibrium configurations, optimal conditions for increasing the frequency non-reciprocity of counter-propagating SWs in Damon-Eshbach configuration are predicted and then confirmed with computer simulations and BLS for a prototype Py/Ir/CoFeB sample. An explicit expression is provided for the frequency shift Δf of two counter-propagating SWs. In the long wavelength limit (small wave-vector k), we find that SW non-reciprocity scales linearly with k, so that an effective DMI constant of dipolar origin can be defined. At intermediate values of k, there is a maximum in Δf that depends only on the thicknesses of the FM layers and non-magnetic spacer, while for larger k, Δf decreases exponentially. Thus, we demonstrate that the proposed bilayer systems exhibit remarkable properties as compared to the widely discussed heavy-metal/ferromagnetic ultrathin systems. In particular, in bilayer systems with antiparallel coupling and in fundamental contrast to DMI-driven systems, non-reciprocity can be notably larger also for thicker FM layers. This opens the possibility to create reconfigurable non-reciprocal devices [18, 74, 75] by controlling the relative magnetic orientation between the coupled FM layers. In the proposed bilayer system, frequency non-reciprocity can be turned on and off simply by switching from antiparallel to parallel magnetization, without any rotation of the applied magnetic field. Such switching can even be controlled and conveniently achieved by applying for example spin-transfer or spin-orbit torques via a local critical current. Moreover, both states, parallel and antiparallel are well-known from GMR and TMR applications and can be tuned to have excellent stability at remanence. Therefore, the bilayer bears a remarkable advantage over other systems, as DMI-driven systems, where reconfigurability can be achieved by rotating the magnetization either in-plane, from DE to backward-volume configuration, or by tipping the magnetization out of the plane [41, 45, 46, 52]. Also, in interfacial DMI systems there is a noticeable increment in magnetic damping due to the heavy metal, which is avoided using a coupled magnetic bilayer. Another advantage is that the bilayer system is compatible to standard deposition processes in the same manner as GMR-stacks are fabricated, and can be integrated into CMOS architectures.

II. THEORY AND SIMULATIONS

A scheme of the considered bilayer system composed of two interacting FM layers (1) and (2) with in-plane magnetization is shown in Fig. 1. Both layers are allowed to exhibit different magnetic parameters and thicknesses d_1 and d_2, while s denotes the separation between them. The equilibrium magnetization of layer $\nu = 1, 2$ makes an angle φ_ν with the z-axis, which is chosen as the propagation direction of the SWs with wave-vector $\mathbf{k} = k\hat{z}$. As we shall see, the non-reciprocity is enhanced in the Damon-Eshbach configuration, particularly in the antiparallel state. Nonetheless, the theory approach accounts for the general case where wave-vector and magnetization may be oriented along an arbitrary direction within the film plane, and moreover accounts for the highly relevant magnetostatic fields created by the dynamic magnetizations.

A. Theory

The LLG equation was linearized and solved with the effective field contribution as explained in the supplemental material [76]. For the symmetric case of two identical FM layers with the same thickness $d_1 = d_2 = d$, being aligned along x but antiparallel (AP) to each other, an analytic formula for the SW dispersion relation for small external fields was derived and reads:

$$f_{\mathrm{m}_1}(k) = \frac{\gamma}{2\pi}\left\{g(k) + \sqrt{[p(k) - g(|k|)]\,[q(k) - g(|k|) - 2C_J]}\right\} \tag{1}$$

$$f_{\mathrm{m}_2}(k) = \frac{\gamma}{2\pi}\left\{-g(k) + \sqrt{[q(k) + g(|k|)]\,[p(k) + g(|k|) - 2C_J]}\right\} \tag{2}$$

where $f_{\mathrm{m}_1}(k)$ and $f_{\mathrm{m}_2}(k)$ correspond to the two modes, namely the acoustic and optical modes, of the bilayer system. In what follows, the mode analyzed will be the

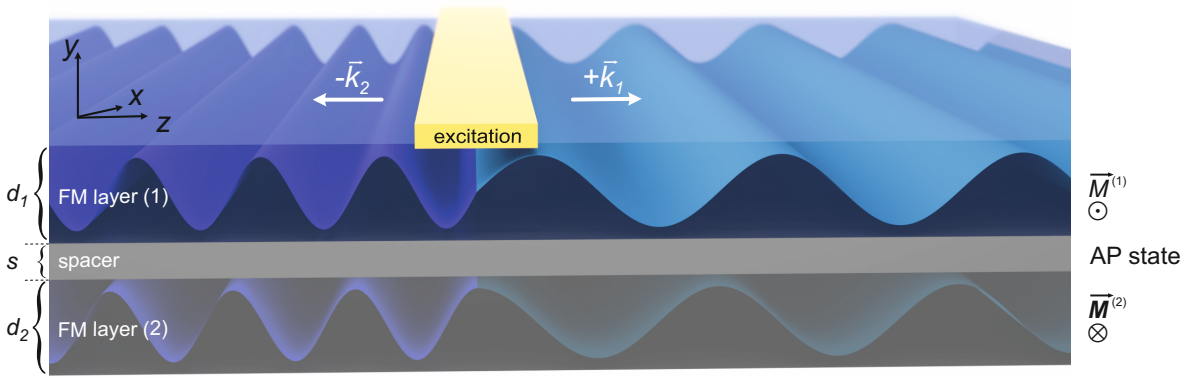

FIG. 1. Overview of the magnetic bilayer system. The static magnetization configuration is in the antiparallel (AP) state. The spin wave is excited below the yellow region, traveling along positive and negative wave-vectors with different wavelength as indicated by the different color of the waves.

low-frequency one that corresponds to $f_{\mathrm{m}_1}(k)$. The individual terms are defined by:

$$g(k) = \mu_0 M_\mathrm{s} \zeta(k)^2 e^{-|k|s} k\, d/2, \tag{3}$$

$$p(k) = \mu_0 H_\mathrm{u} + \mu_0 M_\mathrm{s} k^2 \lambda_\mathrm{ex}^2 + \mu_0 M_\mathrm{s}[1-\zeta(k)], \tag{4}$$

$$q(k) = \mu_0 H_\mathrm{u} - \mu_0 H_\mathrm{s} + \mu_0 M_\mathrm{s} k^2 \lambda_\mathrm{ex}^2 + \mu_0 M_\mathrm{s} \zeta(k), \tag{5}$$

with

$$\zeta(k) = \frac{\sinh(kd/2)}{kd/2} e^{-|k|\frac{d}{2}}, \tag{6}$$

and $C_J = (J_\mathrm{bl} - 2J_\mathrm{bq})/(M_\mathrm{s} d)$. Here, $J_\mathrm{bl}/M_\mathrm{s} d$ ($J_\mathrm{bq}/M_\mathrm{s} d$) is the bilinear (biquadratic) interlayer exchange field, $\mu_0 H_\mathrm{u}$ a possible uniaxial in-plane anisotropy field, M_s the saturation magnetization, λ_ex the exchange length and γ the gyromagnetic ratio. Also, $\mu_0 H_\mathrm{s}$ represents a surface uniaxial anisotropy field, which competes with the static dipolar field allowing to define an effective magnetization $\mu_0 M_\mathrm{eff} = \mu_0 M_\mathrm{s} - \mu_0 H_\mathrm{s}$. The general case, assuming two different FM layers with different magnetic parameters, being more complex, can be solved with the eigenproblem presented in the supplemental material [76].

From Eqs. (1-3) it is clearly visible that it is the term $g(k)$ introducing the non-reciprocity. Only this term changes sign as a function of wave-number k. All other terms $p(k)$, $q(k)$ and $\zeta(k)$, are positive for both wave-vector directions and even bound to 1 for $\zeta(k)$. Then, considering the limit of small wave-numbers, yields

$$f_{\mathrm{m}_1}(k \to 0) = f_{\mathrm{m}_1}(0) - \frac{\gamma\mu_0}{4\pi} M_\mathrm{s} d \left(k + \frac{\gamma\mu_0}{2\pi} \frac{H_\mathrm{u}}{f_{\mathrm{m}_1}(0)} |k| \right) \tag{7}$$

for the low-frequency mode, while the high-frequency one, $f_{\mathrm{m}_2}(k)$, follows a similar behavior (not shown). Upon inspection one may realize that the magnon dispersion relation for the bilayer with antiparallel orientation of both ferromagnetic layers in the limit of small k resembles the well-known asymmetric dispersion of ultrathin magnetic films with DMI [41, 42, 52]. Indeed, the frequency shift becomes $\Delta f_\mathrm{AP} \approx \mu_0\gamma(M_\mathrm{s} d/2\pi)k$, which allows to introduce an effective Dzyaloshinskii-Moriya constant, since the frequency shift in heavy-metal/ferromagnetic interfaces follows the same linear behavior with k. Thus, this effective constant induced in the system is given by $D^\mathrm{Dip} = \mu_0 M_\mathrm{s}^2 d/4$. Due to the dipolar nature of the non-reciprocity induced in the system, the effective constant increases linearly with thickness and quadratically with saturation magnetization. Despite the simplicity of D^Dip, this expression is very practical and useful, as it provides the relevant magnetic parameters to optimize the non-reciprocal system in order to reach the desired properties for application purposes, where the non-reciprocity turns out to be relevant for operations in communications and logic devices [1, 13]. Also, it allows to identify if a bilayer is able to emulate a heavy-metal/ferromagnet system with respect to its non-reciprocal SW propagation. For instance, in bilayers of the type heavy-metal/ferromagnet, it has been found that the Dzyaloshinskii-Moriya constant is around $D^\mathrm{DM} = 0.7$ mJ/m^2 for a ferromagnet of thickness 1.6 nm [46]. Here, we can show that similar properties (i.e. $D^\mathrm{DM} = D^\mathrm{Dip}$) can be reached for the same thickness of the ferromagnet (1.6 nm) if a saturation magnetization of $M_\mathrm{s} = 1190$ kA/m is used. To further increase D^DM it is possible to decrease the film thickness to less than 1 nm [48], which is analogous to increase D^Dip by increasing the thicknesses of both FM layers. This, added to the wide versatility of our system, allows us to establish that a ferromagnetic bilayer is an excellent candidate for non-reciprocal magnonic devices, which due to its simplicity and scalability outperforms other systems proposed for corresponding applications in magnon-based data processing, where, for instance, the control of non-reciprocity allows creating unidirectional caustic spin waves [50] that are relevant for the suppression of cross-interference between devices within a magnonic circuit [57].

In the extended k-regime, we further obtain from

Eqs. (1-2) the following analytical expression for Δf_{AP} of two counter-propagating spin waves:

$$\Delta f_{\mathrm{AP}} = \frac{2\gamma}{\pi}\mu_0 M_{\mathrm{s}} \sinh^2(kd/2)\frac{e^{-|k|(d+s)}}{kd}. \quad (8)$$

Note that Eq. (8) is valid for modes $f_{\mathrm{m}_1}(k)$ and $f_{\mathrm{m}_2}(k)$, in such a way that we predict that both modes present asymmetric dispersion with the same magnitude of the frequency shift. Eq. (8) shows that the interlayer exchange fields are not required for generating the non-reciprocity, neither for small nor large wave-vectors. This demonstrates that the effect is solely resulting from the dynamic dipolar interaction. Interlayer exchange coupling may, however, be used to (i) stabilize the AP alignment and to (ii) influence the accessible frequency range.

B. Micromagnetic simulations

To validate the results of the theory, micromagnetic simulations were performed using the GPU-accelerated code MuMax3 [79]. For this a long magnetic bilayer stripe with length $l = 20\,\mu$m and width $w = 80$ nm was considered. To mimic the thin magnetic film, periodic boundary conditions were applied along the x- and z-directions. The material parameters were chosen according to the ones mentioned in the main text for systems $\mathrm{S_I}$ and $\mathrm{S_{II}}$. Using

$$\mathbf{h} = \tilde{h}\frac{\sin(k_0 z)}{k_0 z}\frac{\sin(2\pi f_0 t)}{2\pi f_0 t}\hat{y} \quad (9)$$

as an external rf-field source, the spin waves are excited with a sinc-pulse in space with a cutoff wavelength $\lambda_0 = 2\pi/k_0 = 9.77$ nm, and in time with a cutoff frequency $f_0 = 50$ GHz. The coordinate system is based on the global coordinate system given in Fig. 1. To reconstruct the SW dispersion relation, the magnetization configuration was stored every 10 ps for 12.5 ns and subsequently Fourier transformed in 2D. Additionally, simulations of the hysteresis loops of in-plane and out-of-plane applied field have been performed. In this context, the total energy and the torque were minimized stepwise at subsequently varying applied field values.

III. EXPERIMENTAL DETAILS

A. Sample preparation

The layer stack Ta(5 nm)/$\mathrm{Co_{40}Fe_{40}B_{20}}$(5.7 nm)/Ir(0.6 nm)/$\mathrm{Ni_{81}Fe_{19}}$(6.7 nm)/Ta cap was prepared on thermally oxidized Si substrates by magnetron sputtering at an Ar partial pressure of 0.35 Pa (2.62 mTorr) at room temperature. The deposition rates of each individual material were pre-calibrated by XRR. An underlayer of Ta (4 nm) was used to improve the adhesion. Ferromagnetic CoFeB and NiFe layers were deposited from alloy targets with the composition of $\mathrm{Co_{40}Fe_{40}B_{20}}$ and $\mathrm{Ni_{81}Fe_{19}}$ (in at. %) respectively (at a deposition rate of 0.3 Å/sec). The ferromagnets were separated by a (non-magnetic) Ir spacer layer to achieve antiferromagnetic alignment at zero field (via RKKY-type coupling). A Ta cap layer was used to provide an oxidation barrier.

B. BLS measurements

To investigate the spin-wave non-reciprocity, Brillouin light scattering (BLS) measurements were performed in the Damon-Eshbach (DE) geometry, i.e. by applying a bias magnetic field in the sample plane but perpendicular to the plane of incidence of the laser beam. This allows for probing the spin waves propagating along the in-plane direction perpendicular to the applied field, i.e. in the DE geometry where non-reciprocity in spin-wave frequency is maximal at room temperature. BLS relies on the inelastic light scattering process due to the interaction of the incident photons with magnons. Conventional 180° back-scattered geometry was used along with the provision of wave-vector selectivity to investigate the spin-wave dispersion relation [80, 81]. Monochromatic light (wavelength $\lambda = 532$ nm and power $P = 65$ mW) from a solid-state laser was focused on the sample surface. In the light scattering process, the total momentum is conserved in the plane of the thin film. As a result, the Stokes (anti-Stokes) peaks in the BLS spectra correspond to the creation (annihilation) of magnons with momentum $k = 4\pi/\lambda \sin\theta$, where λ is the wavelength of the incident laser beam and θ refers to the angle of incidence of the laser. Cross polarizations between the incident and the scattered beams were adopted in order to eliminate any phonon contribution to the scattered light and only the magnon contribution was measured. Subsequently, the frequencies of the scattered light are analyzed using a Sandercock-type six-pass tandem Fabry-Pérot interferometer from JRS scientific instruments [82]. To get well defined BLS spectra for the larger incidence angles, the spectra were obtained after counting photons for several hours. Because of the low frequency in the AP coupled region, the free spectral range (FSR) of 30 GHz (20 GHz) for higher (lower) wave-vector and a 2^{10} multi-channel analyzer were used during the BLS measurement. The frequency resolution is determined by estimating $\mathrm{FSR}/2^{10} \approx 0.05$ GHz (0.02 GHz) for higher (lower) wave-vectors for the Stokes and anti-Stokes peaks of the BLS spectra. The sample magnetization was first saturated by applying a high enough magnetic field of -140 mT followed by reducing the field slowly to the bias magnetic field $\mu_0 H$ and BLS spectra were measured at that field for different values of wave-vector. The maximum value of wave-vector in our experiment is 20.4 rad/μm and the resolution is 2.06 rad/μm. For the first few wave-vectors, the Stokes and anti-Stokes peaks merge with the tail of the elastic peaks and could not be resolved and hence, we present the BLS spectra from $k = 6.1$ rad/μm. The

non-reciprocity in the spin-wave frequency (Δf) was calculated by taking the difference between the anti-Stokes and Stokes peak observed in the BLS spectra. Note that the BLS measurements were performed in conventional way, i.e. by investigating thermally excited spin waves. The effect on frequency non-reciprocity, however, relies solely on the dispersion of the system and is thus not influenced by the exact way of spin-wave excitation.

IV. RESULTS AND DISCUSSION

To illustrate the main findings of the paper, permalloy (Py) and cobalt (Co) layers will be first considered. For Py [assumed as layer (1)], a saturation magnetization $M_s^{(1)} = 658$ kA/m and exchange length $\lambda_{ex}^{(1)} = 5.47$ nm are used, while for Co [layer (2)] the saturation magnetization is $M_s^{(2)} = 1150$ kA/m and $\lambda_{ex}^{(2)} = 5.88$ nm. Also, the gyromagnetic ratio is $\gamma = 1.7587 \times 10^{11}$ rad/Ts, for simplicity assumed to be the same for both layers. Two kinds of bilayer configurations are addressed, a Py/Py bilayer referred to as S_I, and a Co/Py bilayer denoted by S_{II}, for which an uniaxial anisotropy field of $\mu_0 H_u^{(2)} = 69.6$ mT was assumed because of the hexagonal Co layer.

In order to induce an AP alignment between both FM layers, we introduce a $s = 1$ nm spacer, leading to an interlayer exchange coupling constant of $J = -1.5$ mJ/m^2. The spin-wave dispersion relations calculated for different thicknesses of the FM layers for systems S_I and S_{II} are shown in Fig. 2 (a) and (c). Here, the frequency of counter-propagating SWs is calculated as a function of wave-vector k for AP magnetization. Micromagnetic simulations have been performed and are shown by the open symbols. The main deviation between theory and simulation occurs for large wave-vectors, which corresponds to wavelengths of the same order of magnitude as the film thickness, so that the non-homogeneous profile of the dynamic magnetization along the thickness will start having a significant influence on the mode frequencies. In effect, the profile will tend to lower the non-reciprocity, so that the frequencies of the micromagnetic simulation are lower than predicted by theory. In case of the non-symmetric system S_{II} the deviation for large thicknesses occurs already at $k = 0$, because of the strong break of symmetry of the effective field due to the two layers having different magnetic parameters.

Our calculations and simulations for S_I, in the case of parallel orientation of both magnetizations yield a fully reciprocal dispersion. We note, however, that this is not the case for the asymmetric system S_{II}, for which a small non-reciprocity about 0.6 GHz (at $k = 20$ rad/μm) remains even in the P case. Nonetheless, in both cases the non-reciprocity for the antiparallel alignment by far exceeds the one for the parallel alignment, so that via switching between these two configurations the non-reciprocal behavior for spin waves can be turned on and off. This in turn allows for fabricating a non-reciprocal magnonic device that relies solely on the dynamic coupling of the spin waves in the FM bilayer.

In order to understand the physical mechanisms behind the large enhancement of the spin-wave non-reciprocity, the dynamic dipolar stray fields outside and inside of the FM films are carefully analyzed. Figs. 3(a) and (b) depict these fields created by the magnetic charges in the bilayer system for the AP state, where the big arrows represent the orientation of the dynamical magnetization. The main feature of these configurations is that the relative orientation of the dynamical stray field and the dynamical magnetization depend on the static magnetization alignment and the wave-number k. Therefore, the dynamic dipolar interaction energy density $\epsilon_d = -(\mu_0/2)\mathbf{m}\cdot\mathbf{h}^{\text{stray}}$ differs for the presented cases. Here, the distribution of the stray field $\mathbf{h}^{\text{stray}}$ and the dynamical magnetizations for $k > 0$ and $k < 0$ are depicted in Fig. 3. In the AP state with $k > 0$ [Fig. 3(a)] the stray fields and the dynamic magnetizations are always parallel, in such a way that ϵ_d becomes small. Thus, this frequency represents a state of low energy that appears only in the AP configuration. In the configuration shown in Fig. 3(b) ($k < 0$), the stray fields are always opposite to the out-of-plane dynamical magnetization, inducing a higher ϵ_d as compared to the case presented in Fig. 3(a), notably increasing the SW frequencies, and therefore introducing non-reciprocity to the system.

In strong contrast to previously used DMI interactions, the non-reciprocity effects presented here are strongly tunable by the FM layer thickness d, which also affects the maximum frequency difference. Furthermore, in the case of system S_I, it is easy to see that in the limits $d \to 0$ and $d \to \infty$ this frequency asymmetry becomes zero and, thus, there is a particular wave-vector for which Δf_{AP} is maximum, which can be determined from the relation $\tanh\left(\frac{k^* d}{2}\right) = \frac{k^* d}{1+k^*(d+s)}$. Consequently, only the geometry parameters d and s determine the wave-number k^*, for which the largest non-reciprocity is expected. Moreover, it is noted that the maximum frequency shift $\Delta f_{AP}(k^*)$ decays exponentially with the separation of the layers s, and increases with the layer thickness d, due to the dipolar nature of the induced non-reciprocity.

To further validate the presented theory, BLS experiments were performed [6, 28]. Three representative Brillouin light scattering spectra for DE spin waves recorded at selected wave-numbers under an in-plane bias magnetic field ($\mu_0 H = -5$ mT) are shown in Fig. 4(a). According to the vibrating sample magnetometry (conventional VSM) and SQUID-VSM loops, as shown in the supplemental material [76], this corresponds to the antiferromagnetically coupled region for the investigated sample $Co_{40}Fe_{40}B_{20}$ (5.7 nm)/ Ir(0.6 nm)/ $Ni_{81}Fe_{19}$ (6.7 nm), where the thicknesses were estimated from TEM measurements [76]. In order to estimate the frequency difference Δf between counter-propagating spin waves (anti-Stokes and Stokes peaks), the mirror curve of the

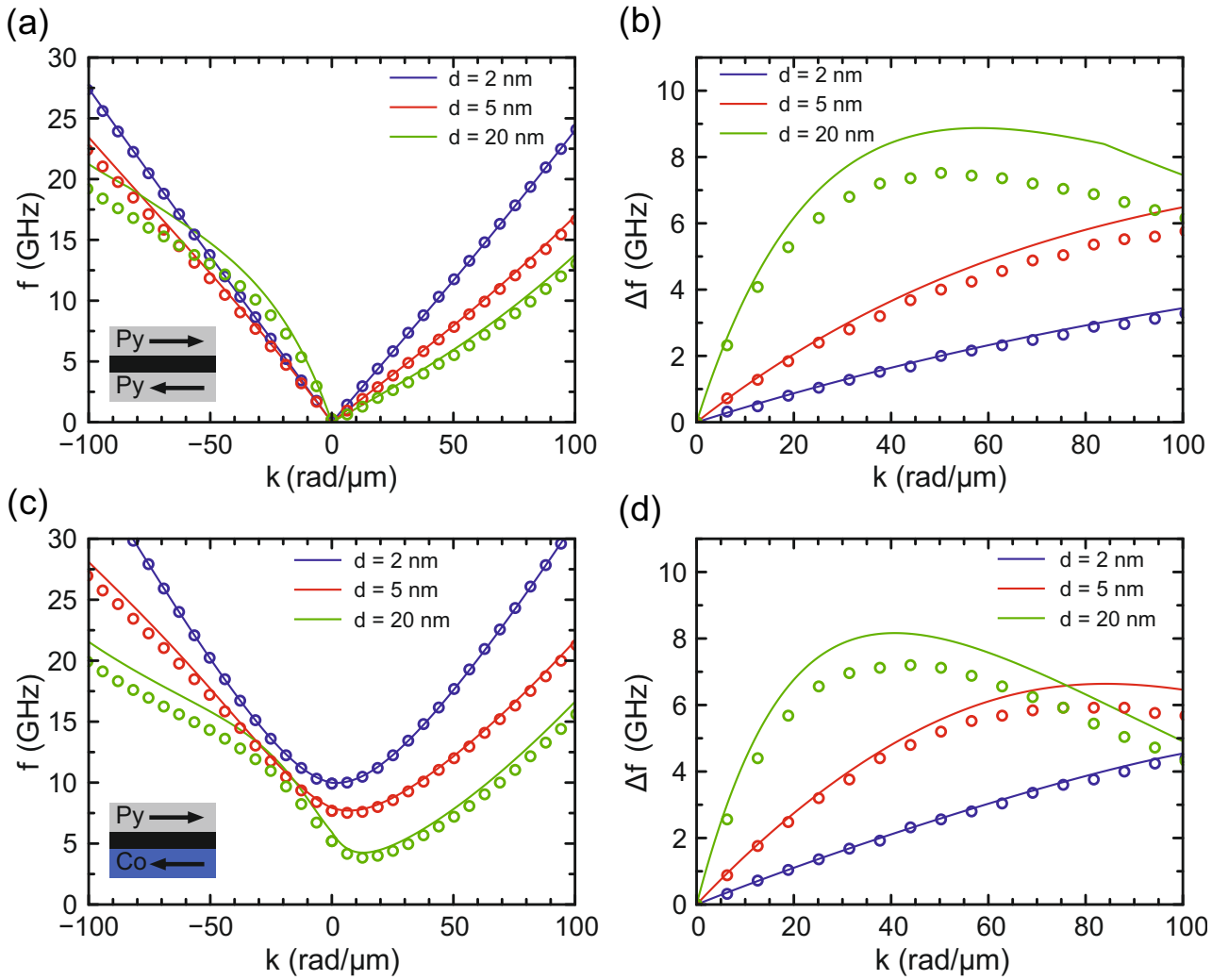

FIG. 2. Non-reciprocal magnon spectrum for coupled ferromagnetic bilayers. (a) Non-reciprocal spin wave dispersion relation for the Py/Py system S_I and (c) for the Py/Co system S_{II}. (b,d) Corresponding frequency shift Δf of two counter-propagating spin waves as a function of the wave-number, for the case of antiparallel equilibrium states of the bilayers. In all plots the open symbols show the results of the micromagnetic simulation and the solid lines depict the theory. The material parameters are given in the main text.

	d (nm)	$\mu_0 M_{\rm eff}$ (mT)	$\mu_0 H_{\rm u}$ (mT)	$J_{\rm bl}$ (mJ/m^2)	$J_{\rm bq}$ (mJ/m^2)	s (nm)
$Ni_{81}Fe_{19}$	6.7	942.5	4.0	-0.195	-0.044	0.6
$Co_{40}Fe_{40}B_{20}$	5.7	1442.9	0.0			

TABLE I. Experimentally determined material parameters. The magnetic properties are determined by FMR, SQUID and conventional VSM. The layer thicknesses and the spacer thickness are determined by cross-section TEM.

anti-Stokes peak has been shown by a blue dotted curve in each spectrum. It is evident that Δf increases with increasing wave-number. The value of Δf attains a maximum of 2.20 GHz at $k = 20.4$ rad/μm. Fig. 4(b) shows the spin-wave dispersion relation measured at $\mu_0 H = -5$ mT. The dispersion relation is asymmetric with respect to the two oppositely propagating spin waves. Shown in Fig. 4(c) is the variation of Δf as a function of k for the AP state.

In order to fit the theoretical model to the experimental data, all the material parameters, besides the exchange constant, were determined experimentally. Ferromagnetic resonance (FMR) experiments were carried out to measure all magnetic properties of the bilayer, such as the effective magnetization $\mu_0 M_{\rm eff}$, the bilinear (biquadratic) interlayer exchange coupling constant $J_{\rm bl}$ ($J_{\rm bq}$) and the anisotropy field $\mu_0 H_{\rm u}$. As already discussed above, both the spacer thickness s and the FM layer thicknesses d are crucial parameters to describe the non-reciprocity. These geometric parameters were determined by trans-

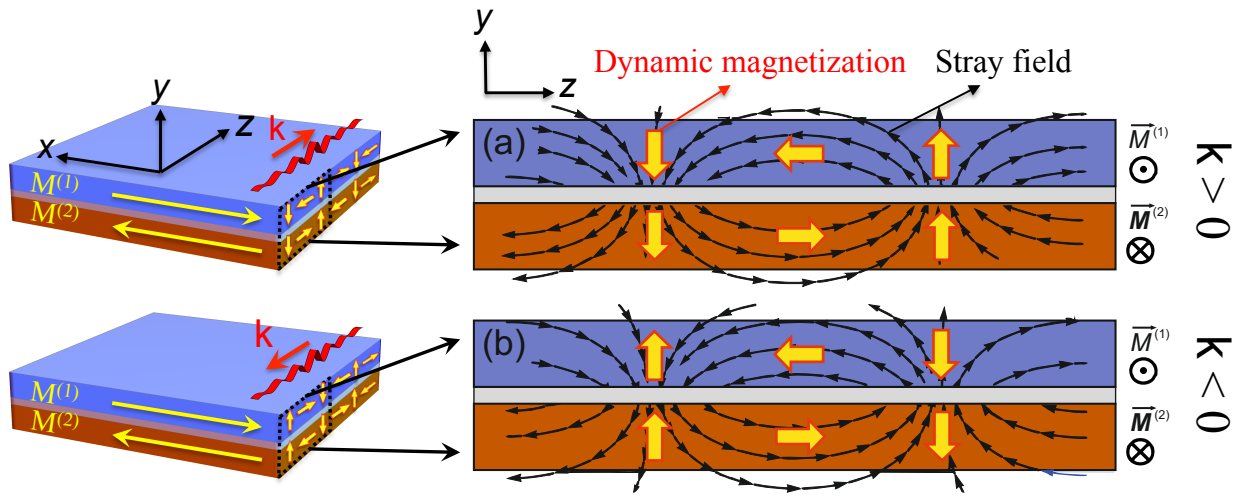

FIG. 3. Dynamic stray fields induced by the surface and volumetric magnetic charges in a ferromagnetic bilayer. The big arrows depict the orientation of the dynamic magnetization, while the static magnetizations are pointing along the $\pm x$. The distributions of dynamic magnetizations and stray fields are shown in (a) $k > 0$ and (b) $k < 0$, for an antiparallel equilibrium state. In agreement with Fig. 2, the lower energy state is obtained for $k > 0$, shown in (a), where dynamic magnetization and stray field are almost parallel.

mission electron microscopy (TEM). The experimentally determined material parameters are listed in table I and further details are provided in the supplemental material [76]. The agreement between the theory and the BLS experiments is good. In Fig. 4(b) it is visible that the positive wave-numbers fit almost perfectly. However, for negative wave-numbers the agreement is somewhat less perfect. To exclude that the material parameters cause this effect, also the spin-wave dispersion for the parallel alignment was measured. The results are shown in the supplementary material [76]. For the P case the agreement is almost perfect. The deviation for the branch at negative k with higher group velocity may be related to the fact that in our system the in-plane anisotropy is rather weak (about mT), so that some small tilting of the two ferromagnetic layers away from the AP alignment is not unlikely, due to a non-vanishing biquadratic coupling contribution. As shown in the supplementary material [76] this scenario is confirmed by magnetometry data. In any case, such small misalignment would lead to a reduction of the non-reciprocity, in particular for higher wave-vector values. A tilting angle of 25° would lead to a reduction of the non-reciprocity of approximately 50%.

CONCLUSIONS

The dynamic magnetic properties of a coupled ferromagnetic bilayer system have been studied. By means of a spin-wave theory, micromagnetic simulations, and Brillouin light scattering measurements, it is demonstrated that the dipolar interaction produced by the dynamic magnetizations between the FM layers is a notable source of non-reciprocity in the spin-wave frequency, with the remarkable property of reconfigurability that relies on the control of the relative magnetic orientation of the interacting FM layers. In the bilayer structures we can have in-plane remanent stable states with a parallel as well as an antiparallel configuration, as is well-known from GMR and TMR applications. Therefore, one can reconfigure the bilayer system reliably into a reciprocal and non-reciprocal device just by the magnetic field history or alternatively by applying a local torque to one of the layers via a critical current density. The change from non-reciprocal to reciprocal spin waves will be more difficult to obtain by switching the magnetization 90° in the plane, or 90° out of the plane, as required in other nonreciprocal systems. Also, in the small wave-vector limit, we show that the bilayer system can emulate the non-reciprocity produced by the Dzyaloshinskii-Moriya interaction in FM/heavy-metal stacks, even for ultra-thin ferromagnetic films. Thus, a bilayer system exhibits the ability to mimic the extensively studied dynamic properties of FM/heavy-metal layers and, at the same time, presents an easy way to control the magnitude of the non-reciprocity by means of the geometry and the equilibrium configuration. These findings open new routes for the creation of nanoscale non-reciprocal magnonic devices and motivate a deeper study of this type of systems, in order to optimize their design according to the desired application requirements.

ACKNOWLEDGMENTS

The authors thank M. Scheinfein and A. Kákay for valuable discussions, and B. Böhm for help with x-ray reflectivity thickness calibrations for sample fabrication.

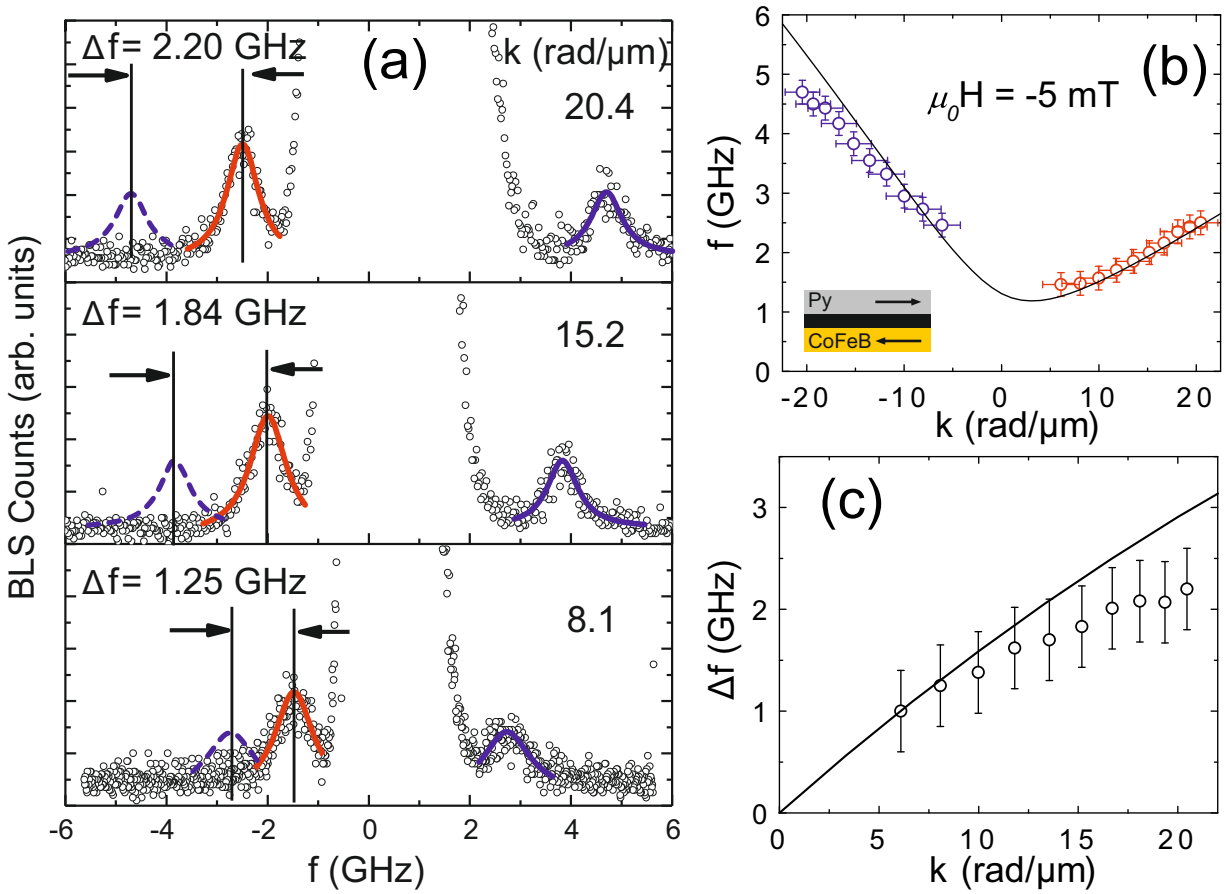

FIG. 4. Representative Brillouin light scattering spectra for Damon-Eshbach spin waves recorded at an external applied field $\mu_0 H = -5$ mT in a $Co_{40}Fe_{40}B_{20}$(5.7 nm)/Ir(0.6 nm)/$Ni_{81}Fe_{19}$(6.7 nm) bilayer sample for two counter-propagating directions. The spectra correspond to a specific wave-vector k as given in each panel. Open symbols are the experimental data points whereas solid curves (red and blue) are the fits using a Lorentzian function. To show the frequency asymmetry (Δf), the mirror curve of the anti-Stokes peak (blue dotted curve) is superimposed. (b) The asymmetric spin-wave dispersion relation measured at $\mu_0 H$ =-5 mT (in antiferromagnetically coupled region). (c) Variation of Δf as a function of k. The solid lines in (b) and (c) correspond to the analytical calculations. Results for the parallel state are shown in the supplementary material [76].

We acknowledge financial support in Chile from FONDECYT 11170736, 1161403, 3170647, and Basal Program for Centers of Excellence, Grant FB0807 CEDENNA, CONICYT. T. S. acknowledges the support by the InProTUC scholarship.

R. A. G. and T. S. contributed equally to this work. R. A. G., A. R. M. and P. L. developed the analytical model. T. S. carried out numerical simulations. A. K. C. and A. B. carried out the BLS measurements. S. S. P. K. A. prepared the sample. A. O. and S. S. P. K. A. carried out the SQUID-VSM and conventional VSM measurements. R. H. carried out the TEM measurements. P. L., K. L., J. L., O. H. and J. F. supervised the project. All authors contributed to writing the manuscript.

[1] A. V. Chumak, V. I. Vasyuchka, A. A. Serga, and B. Hillebrands, "Magnon spintronics," Nat. Phys. **11**, 453 (2015).
[2] G. Gubbiotti, S. Tacchi, G. Carlotti, N. Singh, S. Goolaup, A. O. Adeyeye, and M. Kostylev, "Collective spin modes in monodimensional magnonic crystals consisting of dipolarly coupled nanowires," Appl. Phys. Lett. **90**, 092503 (2007).
[3] K.-S. Lee, D.-S. Han, and S.-K. Kim, "Physical origin and generic control of magnonic band gaps of dipole-exchange spin waves in width-modulated nanostrip waveguides," Phys. Rev. Lett. **102**, 127202 (2009).
[4] S. Neusser and D. Grundler, "Magnonics: Spin waves on the nanoscale," Adv. Mat. **21**, 2927 (2009).

[5] A. A. Serga, A. V. Chumak, and B. Hillebrands, "YIG magnonics," J. Phys. D: Appl. Phys. **43**, 264002 (2010).

[6] G. Gubbiotti, S. Tacchi, M. Madami, G. Carlotti, A. O. Adeyeye, and M. Kostylev, "Brillouin light scattering studies of planar metallic magnonic crystals," J. Phys. D: Appl. Phys. **43**, 264003 (2010).

[7] Z. K. Wang, V. L. Zhang, H. S. Lim, S. C. Ng, M. H. Kuok, S. Jain, and A. O. Adeyeye, "Nanostructured magnonic crystals with size-tunable bandgaps," ACS Nano **4**, 643 (2010).

[8] J. Ding, M. Kostylev, and A. O. Adeyeye, "Magnetic hysteresis of dynamic response of one-dimensional magnonic crystals consisting of homogenous and alternating width nanowires observed with broadband ferromagnetic resonance," Phys. Rev. B **84**, 054425 (2011).

[9] S. Tacchi, G. Duerr, J. W. Klos, M. Madami, S. Neusser, G. Gubbiotti, G. Carlotti, M. Krawczyk, and D. Grundler, "Forbidden band gaps in the spin-wave spectrum of a two-dimensional bicomponent magnonic crystal," Phys. Rev. Lett. **109**, 137202 (2012).

[10] S.-K. Kim, K.-S. Lee, and D.-S. Han, "A gigahertz-range spin-wave filter composed of width-modulated nanostrip magnonic-crystal waveguides," Appl. Phys. Lett. **95**, 082507 (2009).

[11] A. V. Chumak, V. I. Vasyuchka, A. A. Serga, M. P. Kostylev, V. S. Tiberkevich, and B. Hillebrands, "Storage-recovery phenomenon in magnonic crystal," Phys. Rev. Lett. **108**, 257207 (2012).

[12] H. Yu, G. Duerr, R. Huber, M. Bahr, T. Schwarze, F. Brandl, and D. Grundler, "Omnidirectional spin-wave nanograting coupler," Nat. Commun. **4**, 2702 (2013).

[13] M. Jamali, J. H. Kwon, S.-M. Seo, K.-J. Lee, and H. Yang, "Spin wave nonreciprocity for logic device applications," Sci. Rep. **3**, 3160 (2013).

[14] A. V. Chumak, A. A. Serga, and B. Hillebrands, "Magnon transistor for all-magnon data processing," Nat. Commun. **5**, 4700 (2014).

[15] T. Brächer, F. Heussner, P. Pirro, T. Meyer, T. Fischer, M. Geilen, B. Heinz, B. Lägel, A. A. Serga, and B. Hillebrands, "Phase-to-intensity conversion of magnonic spin currents and application to the design of a majority gate," Sci. Rep. **6**, 38235 (2016).

[16] B. Rana and Y. C. Otani, "Voltage-controlled reconfigurable spin-wave nanochannels and logic devices," Phys. Rev. Appl. **9**, 014033 (2018).

[17] A. V. Sadovnikov, V. A. Gubanov, S. E. Sheshukova, Yu. P. Sharaevskii, and S. A. Nikitov, "Spin-wave drop filter based on asymmetric side-coupled magnonic crystals," Phys. Rev. Appl. **9**, 051002 (2018).

[18] R. E. Camley, "Nonreciprocal surface waves," Surf. Sci. Rep. **7**, 103 (1987).

[19] J. Lan, W. Yu, R. Wu, and J. Xiao, "Spin-wave diode," Phys. Rev. X **5**, 041049 (2015).

[20] X. S. Wang, H. W. Zhang, and X. R. Wang, "Topological magnonics: A paradigm for spin-wave manipulation and device design," Phys. Rev. Appl. **9**, 024029 (2018).

[21] N. Reiskarimian and H. Krishnaswamy, "Magnetic-free non-reciprocity based on staggered commutation," Nat. Commun. **7**, 11217 (2016).

[22] D. L. Sounas and A. Alù, "Non-reciprocal photonics based on time modulation," Nat. Photonics **11**, 774 (2017).

[23] R. W. Damon and J. R. Eshbach, "Magnetostatic modes of a ferromagnet slab," J. Phys. Chem. Solids **19**, 308 (1961).

[24] L. K. Brundle and N. J. Freedman, "Magnetostatic surface waves on a y.i.g. slab," Electron. Lett. **4**, 132 (1968).

[25] T. Wolfram and R. E. DeWames, "Surface dynamics of magnetic materials," Prog. Surf. Sci. **2**, 233 (1972).

[26] V. E. Demidov, M. P. Kostylev, K. Rott, P. Krzysteczko, G. Reiss, and S. O. Demokritov, "Excitation of microwaveguide modes by a stripe antenna," Appl. Phys. Lett. **95**, 112509 (2009).

[27] B. Hillebrands, "Spin-wave calculations for multilayered structures," Phys. Rev. B **41**, 530 (1990).

[28] B. Hillebrands, "Light scattering in solids vii: Crystal-field and magnetic excitations," (Springer, Berlin, Heidelberg, 2000) pp. 174–289.

[29] P. K. Amiri, B. Rejaei, M. Vroubel, and Y. Zhuang, "Nonreciprocal spin wave spectroscopy of thin Ni–Fe stripes," Appl. Phys. Lett. **91**, 062502 (2007).

[30] M. Mruczkiewicz, M. Krawczyk, G. Gubbiotti, S. Tacchi, Yu. A. Filimonov, D. V. Kalyabin, I. V. Lisenkov, and S. A. Nikitov, "Nonreciprocity of spin waves in metallized magnonic crystal," New J. Phys. **15**, 113023 (2013).

[31] M. Mruczkiewicz, E. S. Pavlov, S. L. Vysotsky, M. Krawczyk, Yu. A. Filimonov, and S. A. Nikitov, "Observation of magnonic band gaps in magnonic crystals with nonreciprocal dispersion relation," Phys. Rev. B **90**, 174416 (2014).

[32] O. Gladii, M. Haidar, Y. Henry, M. Kostylev, and M. Bailleul, "Frequency nonreciprocity of surface spin wave in permalloy thin films," Phys. Rev. B **93**, 054430 (2016).

[33] K. Di, H. S. Lim, V. L. Zhang, S. C. Ng, and M. H. Kuok, "Spin-wave nonreciprocity based on interband magnonic transitions," Appl. Phys. Lett. **103**, 132401 (2013).

[34] I. Dzyaloshinsky, "A thermodynamic theory of "weak" ferromagnetism of antiferromagnetics," J. Phys. Chem. Solids **4**, 241 (1958).

[35] T. Moriya, "New mechanism of anisotropic superexchange interaction," Phys. Rev. Lett. **4**, 228 (1960).

[36] A. Fert and P. M. Levy, "Role of anisotropic exchange interactions in determining the properties of spin-glasses," Phys. Rev. Lett. **44**, 1538–1541 (1980).

[37] N. Nagaosa and Y. Tokura, "Topological properties and dynamics of magnetic skyrmions," Nat. Nanotech. **8**, 899 (2013).

[38] L. Udvardi and L. Szunyogh, "Chiral asymmetry of the spin-wave spectra in ultrathin magnetic films," Phys. Rev. Lett. **102**, 207204 (2009).

[39] Kh. Zakeri, Y. Zhang, J. Prokop, T.-H. Chuang, N. Sakr, W. X. Tang, and J. Kirschner, "Asymmetric spin-wave dispersion on Fe(110): Direct evidence of the Dzyaloshinskii-Moriya interaction," Phys. Rev. Lett. **104**, 137203 (2010).

[40] A. T. Costa, R. B. Muniz, S. Lounis, A. B. Klautau, and D. L. Mills, "Spin-orbit coupling and spin waves in ultrathin ferromagnets: The spin-wave Rashba effect," Phys. Rev. B **82**, 014428 (2010).

[41] D. Cortés-Ortuño and P. Landeros, "Influence of the Dzyaloshinskii-Moriya interaction on the spin-wave spectra of thin films," J. Phys: Condens. Matter **25**, 156001 (2013).

[42] J.-H. Moon, S.-M. Seo, K.-J. Lee, K.-W. Kim, J. Ryu, H.-W. Lee, R. D. McMichael, and M. D. Stiles, "Spin-wave propagation in the presence of interfacial Dzyaloshinskii-Moriya interaction," Phys. Rev. B **88**, 184404 (2013).

[43] K. Di, V. L. Zhang, H. S. Lim, S. C. Ng, M. H. Kuok, X. Qiu, and H. Yang, "Asymmetric spin-wave dispersion due to Dzyaloshinskii-Moriya interaction in an ultrathin Pt/CoFeB film," Appl. Phys. Lett. **106**, 052403 (2015).

[44] K. Di, V. L. Zhang, H. S. Lim, S. C. Ng, M. H. Kuok, J. Yu, J. Yoon, X. Qiu, and H. Yang, "Direct observation of the Dzyaloshinskii-Moriya interaction in a Pt/Co/Ni film," Phys. Rev. Lett. **114**, 047201 (2015).

[45] V. L. Zhang, K. Di, H. S. Lim, S. C. Ng, M. H. Kuok, J. Yu, J. Yoon, X. Qiu, and H. Yang, "In-plane angular dependence of the spin-wave nonreciprocity of an ultrathin film with Dzyaloshinskii-Moriya interaction," Appl. Phys. Lett. **107**, 022402 (2015).

[46] J. Cho, N.-H. Kim, S. Lee, J.-S. Kim, R. Lavrijsen, A. Solignac, Y. Yin, D.-S. Han, N. J. J. van Hoof, H. J. M. Swagten, B. Koopmans, and C.-Y. You, "Thickness dependence of the interfacial Dzyaloshinskii-Moriya interaction in inversion symmetry broken systems," Nat. Commun. **6** (2015).

[47] H. T. Nembach, J. M. Shaw, M. Weiler, E. Jue, and T. J. Silva, "Linear relation between heisenberg exchange and interfacial Dzyaloshinskii-Moriya interaction in metal films," Nat. Phys. **11**, 825 (2015).

[48] M. Belmeguenai, J.-P. Adam, Y. Roussigné, S. Eimer, T. Devolder, J.-V. Kim, S. M. Cherif, A. Stashkevich, and A. Thiaville, "Interfacial Dzyaloshinskii-Moriya interaction in perpendicularly magnetized Pt/Co/AlO_x ultrathin films measured by Brillouin light spectroscopy," Phys. Rev. B **91**, 180405(R) (2015).

[49] A. A. Stashkevich, M. Belmeguenai, Y. Roussigné, S. M. Cherif, M. Kostylev, M. Gabor, D. Lacour, C. Tiusan, and M. Hehn, "Experimental study of spin-wave dispersion in Py/Pt film structures in the presence of an interface Dzyaloshinskii-Moriya interaction," Phys. Rev. B **91**, 214409 (2015).

[50] N.-H. Kim, J. Jung, J. Cho, D.-S. Han, Y. Yin, J.-S. Kim, H. J. M. Swagten, and C.-Y. You, "Interfacial Dzyaloshinskii-Moriya interaction, surface anisotropy energy, and spin pumping at spin orbit coupled Ir/Co interface," Appl. Phys. Lett. **108**, 142406 (2016).

[51] J. M. Lee, C. Jang, B.-Chul Min, S.-W. Lee, K.-J. Lee, and J. Chang, "All-electrical measurement of interfacial Dzyaloshinskii-Moriya interaction using collective spin-wave dynamics," Nano Lett. **16**, 62 (2016).

[52] S. Tacchi, R. E. Troncoso, M. Ahlberg, G. Gubbiotti, M. Madami, J. Åkerman, and P. Landeros, "Interfacial Dzyaloshinskii-Moriya interaction in Pt/CoFeB films: Effect of the heavy-metal thickness," Phys. Rev. Lett. **118**, 147201 (2017).

[53] R. A. Gallardo, D. Cortés-Ortuño, T. Schneider, A. Roldán-Molina, F. Ma, R. E. Troncoso, K. Lenz, H. Fangohr, J. Lindner, and P. Landeros, "Flat bands, indirect gaps, and unconventional spin-wave behavior induced by a periodic Dzyaloshinskii-Moriya interaction," Phys. Rev. Lett. **122**, 067204 (2019).

[54] R. A. Gallardo, D. Cortés-Ortuño, R. E. Troncoso, and P. Landeros, "Three-dimensional magnonics," (Jenny Stanford Publishing, Berlin, Heidelberg, 2019) pp. 121–160.

[55] R. Verba, V. Tiberkevich, E. Bankowski, T. Meitzler, G. Melkov, and A. Slavin, "Conditions for the spin wave nonreciprocity in an array of dipolarly coupled magnetic nanopillars," Appl. Phys. Lett. **103**, 082407 (2013).

[56] J. A. Otálora, M. Yan, H. Schultheiss, R. Hertel, and A. Kákay, "Curvature-induced asymmetric spin-wave dispersion," Phys. Rev. Lett. **117**, 227203 (2016).

[57] K. Di, S. X. Feng, S. N. Piramanayagam, V. L. Zhang, H. S. Lim, S. C. Ng, and M. H. Kuok, "Enhancement of spin-wave nonreciprocity in magnonic crystals via synthetic antiferromagnetic coupling," Sci. Rep. **5**, 10153 (2015).

[58] M. Mruczkiewicz, P. Graczyk, P. Lupo, A. Adeyeye, G. Gubbiotti, and M. Krawczyk, "Spin-wave nonreciprocity and magnonic band structure in a thin permalloy film induced by dynamical coupling with an array of Ni stripes," Phys. Rev. B **96**, 104411 (2017).

[59] S. Wintz, V. Tiberkevich, M. Weigand, J. Raabe, J. Lindner, A. Erbe, A. Slavin, and J. Fassbender, "Magnetic vortex cores as tunable spin-wave emitters," Nat. Nanotechnol. **11**, 948 (2016).

[60] V. Sluka, T. Schneider, R. A. Gallardo, A. Kákay, M. Weigand, T. Warnatz, R. Mattheis, A. Roldán-Molina, P. Landeros, V. Tiberkevich, A. Slavin, G. Schütz, A. Erbe, A. Deac, J. Lindner, J. Raabe, J. Fassbender, and S. Wintz, "Emission and propagation of 1d and 2d spin waves with nanoscale wavelengths in anisotropic spin textures," Nat. Nanotech. **14**, 328 (2019).

[61] M. N. Baibich, J. M. Broto, A. Fert, F. Nguyen Van Dau, F. Petroff, P. Etienne, G. Creuzet, A. Friederich, and J. Chazelas, "Giant magnetoresistance of (001)Fe/(001)Cr magnetic superlattices," Phys. Rev. Lett. **61**, 2472 (1988).

[62] A. Fert, "Nobel lecture: Origin, development, and future of spintronics," Rev. Mod. Phys. **80**, 1517 (2008).

[63] P. A. Grünberg, "Nobel lecture: From spin waves to giant magnetoresistance and beyond," Rev. Mod. Phys. **80**, 1531 (2008).

[64] P. Grünberg, "Some ways to modify the spin-wave mode spectra of magnetic multilayers (invited)," J. Appl. Phys. **57**, 3673 (1985).

[65] P. Grünberg, R. Schreiber, Y. Pang, M. B. Brodsky, and H. Sowers, "Layered magnetic structures: Evidence for antiferromagnetic coupling of Fe layers across Cr interlayers," Phys. Rev. Lett. **57**, 2442 (1986).

[66] P. X. Zhang and W. Zinn, "Spin-wave modes in antiparallel magnetized ferromagnetic double layers," Phys. Rev. B **35**, 5219 (1987).

[67] G. Binasch, P. Grünberg, F. Saurenbach, and W. Zinn, "Enhanced magnetoresistance in layered magnetic structures with antiferromagnetic interlayer exchange," Phys. Rev. B **39**, 4828 (1989).

[68] M. Vohl, J. Barnaś, and P. Grünberg, "Effect of interlayer exchange coupling on spin-wave spectra in magnetic double layers: Theory and experiment," Phys. Rev. B **39**, 12003 (1989).

[69] R. E. Camley and A. A. Maradudin, "Magnetostatic interface waves in ferromagnets," Solid State Commun. **41**, 585 (1982).

[70] K. Mika and P. Grünberg, "Dipolar spin-wave modes of a ferromagnetic multilayer with alternating directions of magnetization," Phys. Rev. B **31**, 4465 (1985).

[71] P. Grünberg and K. Mika, "Magnetostatic spin-wave modes of a ferromagnetic multilayer," Phys. Rev. B **27**, 2955 (1983).

[72] R. L. Stamps and R. E. Camley, "Magnetostatic modes in thin film antiferromagnet/ferromagnet layered systems," J. Magn. Magn. Mater. **54**, 803 (1986).

[73] J. Barnaś and P. Grünberg, "Spin waves in exchange-coupled epitaxial double-layers," J. Magn. Magn. Mater. **82**, 186 (1989).

[74] N. R. Bernier, L. D. Tóth, A. Koottandavida, M. A. Ioannou, D. Malz, A. Nunnenkamp, A. K. Feofanov, and T. J. Kippenberg, "Nonreciprocal reconfigurable microwave optomechanical circuit," Nat. Commun. **8**, 604 (2017).

[75] Z. Shen, Y.-L. Zhang, Y. Chen, F.-W. Sun, X.-B. Zou, G.-C. Guo, C.-L. Zou, and C.-H. Dong, "Reconfigurable optomechanical circulator and directional amplifier," Nat. Commun. **9**, 1797 (2018).

[76] See Supplemental Material at [URL will be inserted by publisher] for a brief description of the theoretical and experimental techniques used in the manuscript, which includes Refs. [77, 78]. .

[77] S. Y. Jang, S. H. Lim, and S. R. Lee, "Magnetic dead layer in amorphous CoFeB layers with various top and bottom structures," J. Appl. Phys. **107**, 09C707 (2010).

[78] H. T. Nembach, T. J. Silva, J. M. Shaw, M. L. Schneider, M. J. Carey, S. Maat, and J. R. Childress, "Perpendicular ferromagnetic resonance measurements of damping and landé g–factor in sputtered $(Co_2Mn)_{1-x}Ge_x$ thin films," Phys. Rev. B **84**, 054424 (2011).

[79] A. Vansteenkiste, J. Leliaert, M. Dvornik, M. Helsen, F. Garcia-Sanchez, and B. Van Waeyenberge, "The design and verification of MuMax3," AIP Advances **4**, 107133 (2014).

[80] A. K. Chaurasiya, C. Banerjee, S. Pan, S. Sahoo, S. Choudhury, J. Sinha, and A. Barman, "Direct observation of interfacial Dzyaloshinskii-Moriya interaction from asymmetric spin-wave propagation in $W/CoFeB/SiO_2$ heterostructures down to sub-nanometer CoFeB thickness," Sci. Rep. **6**, 32592 (2016).

[81] A. K. Chaurasiya, S. Choudhury, J. Sinha, and A. Barman, "Dependence of interfacial Dzyaloshinskii-Moriya interaction on layer thicknesses in $Ta/CoFeB/TaO_x$ heterostructures from Brillouin light scattering," Phys. Rev. Appl. **9**, 014008 (2018).

[82] R. Mock, B. Hillebrands, and R. Sandercock, "Construction and performance of a Brillouin scattering set-up using a triple-pass tandem Fabry-Perot interferometer," J. Phys. E: Sci. Instrum. **20**, 656 (1987).